Journal of Functional Materials and Applied Engineering

Research Paper

Study on the Removal of Trace Organic Matter from Water by the Ozone-Activated Carbon (O3/C) Process

David Narr [1], **Tahar Novoa** [1], **Carlos Pandey** [2,*]

[1] Université de Sfax, Ecole Nationale d'Ingénieurs de Sfax, Laboratoire de Biochimie et de Génie Enzymatique des Lipases, 3038 Sfax, Tunisia
[2] Department of Chemistry, University of Utah, 315 South 1400 East, Salt Lake City, UT, 84112, USA
*Corresponding author: Carlos.Pandey@utah.edu

Abstract. Owing to the complex structure and low biodegradability of most trace organic compounds found in source water, the removal efficiency of these contaminants by the O_3-C process declines correspondingly once the adsorption capacity of the activated carbon is exhausted. In the O_3/C process, however, the surface morphology and pore structure of the activated carbon remain largely intact after extended operation. There is only a minor reduction in specific surface area and micropore volume, and its adsorption capacity remains comparable to that of fresh activated carbon; whereas in the O3-C process, the surface pore structure of activated carbon is covered by a dense, uniform layer of pollutants, the adsorption capacity decreases by nearly 75%, and a large number of short rod-shaped bacteria are present on the activated carbon surface, indicating that it has transformed into biological activated carbon, thereby almost losing the adsorption function of activated carbon. This indicates that the O3/C process can prolong the adsorption performance of activated carbon. BET test results showed that continuous ozone oxidation of activated carbon can lead to an increase in the proportion of micropore volume, indicating that ozone contact oxidation has a certain destructive effect on the macropores and mesopores of activated carbon. O_3/C outperforms O_3-C because activated carbon catalyses ozone to generate strongly oxidising •OH and HO_2• radicals; additionally, dissolved O_3 is converted to H_2O_2 on the carbon surface. The decomposition of H2O2 can produce additional HO2•, increasing the production of •OH in the O3/C process and improving the oxidation effect. Ozone–carbon contact produces abundant •OH that oxidises organics and biofilm coating the carbon surface, liberating active sites and accomplishing in-situ carbon regeneration. Through optimized process design, improved equipment efficiency, and strengthened operation management, the O3/C process significantly reduces overall operating costs in three aspects: synchronous regeneration of activated carbon, high ozone utilization rate, and reduced secondary lifting, achieving economically efficient operation goals.

Keywords: *Micro-pollutant removal; Ozone treatment; Activated carbon treatment*

Received on 12 June 2025, Accepted on 05 Nov 2025, Published on 15 Dec 2025

1 Introduction

Micro-polluted source water primarily consists of organic pollutants. Currently, to achieve the goal of removing micro-pollutants from water, methods such as enhanced pretreatment and advanced treatment are generally adopted. Enhanced pretreatment includes biological pretreatment, advanced oxidation pretreatment, activated carbon adsorption, etc. Enhanced pretreatment can oxidize, decompose, or adsorb trace organic matter in water at the front end of the water treatment process, reducing the treatment load of subsequent conventional processes. Its advantages are good effectiveness and process flexibility. However, the drawback of pretreatment is that it often produces certain oxidation intermediate products. If these intermediate products cannot be effectively removed in subsequent processes, new water quality issues will arise. Another approach is to add advanced treatment processes after conventional processes, such as membrane technology and ozone-activated carbon technology. Advanced treatment processes have the advantages of stable treatment effects and guaranteed effluent quality. However, the currently used membrane technology and ozone-activated carbon technology have certain operational management issues in practice, requiring process optimization.

To comply with increasingly stringent drinking water quality regulations, ozone-activated carbon integrated technology has been widely adopted in advanced treatment systems at water treatment plants. The presence of organic matter in water exerts a protective effect on colloidal particles, enhancing their stability and consequently increasing the complexity of water treatment. High ammonia nitrogen values affect coagulation efficiency, produce odors, and after chlorination disinfection, they easily combine with humic substances in the raw water to form disinfection by-products such as organic halides, directly threatening human health. Conventional trains are inherently constrained in eliminating dissolved trace organics because of their limited purification mechanisms . Therefore, water treatment plants need to add advanced treatment processes on the basis of conventional processes to ensure effluent quality. Currently, commonly used advanced treatment processes mainly include advanced oxidation (including Fenton, UV, UV/Cl, etc.) technology, membrane technology, and ozone-biological activated carbon process. As mentioned earlier, advanced oxidation technology and membrane technology still have problems in practical applications, such as complex pretreatment, high cost, high energy consumption, and treatment efficiency being affected by water quality factors, making large-scale application difficult [2].

The ozone-activated carbon (O_3-AC) process is currently the most extensively utilized technology in advanced water treatment. Since the 1980s, it has been applied to address challenges such as micro-polluted source water [3], demonstrating effective treatment performance. The ozone-activated carbon process integrates four technologies: physical-chemical adsorption by activated carbon, ozone oxidation, biodegradation, and ozone disinfection. Its main functions include removing color and odor substances from water, removing micro-pollutant organic matter, reducing the formation potential of disinfection by-products, and improving the biological stability of effluent. Ozone attacks π-electron clouds of aromatics and alkenes, grafting –OH, –COOH or C=O fragments that turn hydrophobic skeletons into water-friendly motifs; the cleavage shrinks aromaticity, breaks large stubborn chains into bite-size, labile species and primes the effluent for far better activated-carbon uptake downstream. Ozone-activated carbon has now become the preferred process for solving water color and odor problems, controlling disinfection by-products, and improving water biological stability [6].

As an advanced water treatment technology, during the operation of the ozone-activated carbon (O_3-AC) process, the activated carbon filter accumulates significant dissolved oxygen from ozone decomposition along with adsorbed and concentrated organic compounds. This environment inevitably promotes the proliferation of microorganisms on the surface of the activated carbon. Eventually, the activated carbon, which primarily functioned by adsorption, transforms into biological activated carbon dominated by biodegradation. The proliferation of microorganisms on the activated carbon surface results in a reduction of its effective area and a rapid decrease in adsorption capacity. Given that most trace organic compounds in water possess complex structures and low biodegradability, the removal efficiency of the ozone-biological activated carbon process for these contaminants diminishes as the adsorption capacity of the carbon declines. To sustain the adsorption performance of the activated carbon, the oxidizing action of ozone can be utilized to suppress microbial growth on its surface. This helps prolong the adsorption capability of the activated carbon and maintains the effectiveness of the ozone-activated carbon combined process in removing recalcitrant trace organic matter from micro-polluted source water. Mao et al. [7] reported that ozonation effectively dismantles recalcitrant organics while spawning polar by-products; yet these water-loving fragments tend to be repelled by the hydrophobic carbon surface. To offset this mismatch, researchers have merged oxidation and sorption into one vessel, creating a hybrid O_3/GAC system where ozone and activated carbon work concurrently. While removing organic pollutants, it indirectly achieves regeneration of activated carbon, extending the service life of activated carbon. Liu et al. [8] used an integrated ozone-activated carbon device to remove atrazine and observed the synchronous regeneration effect of activated carbon. The unified O_3–carbon reactor delivered 99.9 % atrazine elimination, far outpacing stand-alone carbon revival tactics—ozone-stream and ozone-soak methods merely restored 52.9 % and 49.0 % of the adsorbent's capacity, respectively. The removal rates of atrazine by the regenerated activated carbon were 39.2% and 36.4%, respectively. After 90 days of operation, the atrazine removal rate of the O3 synchronously regenerated activated carbon could still reach 70%.

Additionally, since activated carbon can initiate the reaction of ozone to generate •OH free radicals, the presence of activated carbon during ozone oxidation enhances the oxidation effect. This synergistic effect between ozone and activated carbon is called carbon-based catalytic ozonation [9]. Through this effect, activated carbon not only utilizes its high adsorption performance to effectively remove •OH free radical quenchers but also improves the ability and quantity of ozone to generate •OH free radicals. Moreover, it can act as an initiator and promoter of the O3 advanced oxidation chain reaction, strengthening the performance of indirect oxidation by O3, thereby improving the oxidation performance of organic matter in water.

In the integrated ozone-activated carbon (O_3-AC) process, ozone oxidation can modify the surface properties of the activated carbon, particularly its pore structure, specific surface area, and surface functional groups, thereby helping to restore the adsorption capacity of the activated carbon. Therefore, in the integrated process, using the oxidizing effect of ozone to generate highly active and strongly oxidizing •OH free radicals, •OH can oxidize and degrade organic and some inorganic pollutants in the pores of activated carbon, ultimately generating substances such as CO2 and H2O, enabling the regeneration of saturated activated carbon [10]. Ye et al. [11] found that the regeneration rate of modified activated carbon by •OH was 88%. Zhu Jinfeng et al. [55] used ultrasound to generate •OH free radicals to regenerate activated carbon, achieving a regeneration rate of 86.1%. C. TRELLU et al. [12] leveraged an advanced oxidation route to reclaim phenol-laden carbon, reviving roughly 70 % of its uptake power [13], underscoring that wedding ozone to the carbon bed fleshes out a single-stage cycle where pollutant destruction and sorbent renewal proceed in lockstep. The online synchronous regeneration effect of activated carbon by ozone is achieved, extending the adsorption capacity and service life of activated carbon.

This study used three organic compounds with different solubilities and biodegradabilities in water—phenol, Rhodamine B (RhB), and humic acid—as representative pollutants to investigate the removal effects of two different ozone-activated carbon combination processes on these three pollutants. An integrated ozone-activated carbon (O_3-AC) system was constructed, consolidating the two sequential stages of ozone oxidation and activated carbon adsorption from the conventional O_3-AC process into a single unit operation. The removal performance and operational stability of the traditional O_3-AC process and the integrated O_3-AC system were compared.

2 Experimental Process

2.1 Wastewater Preparation

The phenol solution used in the experiment was prepared using pure water as a stock solution. The prepared phenol stock solution had a mass concentration of 5000 mg/L. Accurately weigh 5g of phenol using an analytical balance, transfer the dissolved phenol solution to a volumetric flask, and make up to 1L volume. The prepared phenol stock solution is stored in a cool place for later use. When needed, take a specific amount of the stock solution and dilute it to obtain the raw water with the required phenol concentration.

The RhB used in the experiment was prepared using pure water as a stock solution. A 3 g L^{-1} RhB master liquor was prepared for subsequent tests. Accurately weigh 3g of RhB using an analytical balance, transfer the dissolved RhB solution to a volumetric flask, and make up to 1L volume. The prepared RhB stock solution is stored in a cool, dark place for later use. When needed, take a specific amount of the stock solution and dilute it to obtain the required RhB concentration raw water.

The humic acid used in the experiment was prepared using pure water as a stock solution. The prepared humic acid stock solution had a mass concentration of 5000 mg/L. Accurately weigh 5g of dried humic acid powder, fully dissolve it in pure water under alkaline conditions with stirring, transfer the dissolved humic acid solution to a volumetric flask, and make up to 1L volume. Take a specific amount of the stock solution and dilute it to obtain the required humic acid concentration raw water, then adjust the pH to neutral using dilute hydrochloric acid.

The ammonia nitrogen solution used in the experiment was prepared using ammonium chloride. The ammonium chloride used in the experiment was prepared using pure water as a stock solution. The prepared ammonium chloride stock solution had a mass concentration of 3000 mg/L. Accurately weigh 3g of ammonium chloride, transfer the dissolved ammonium chloride solution to a volumetric flask, and make up to 1L volume. The prepared ammonium chloride stock solution is stored in a cool place for later use. Each time, only a specific amount of the stock solution needs to be diluted to obtain the required ammonium chloride concentration raw water.

2.2 Experimental Setup

The experimental apparatus consisted of an ozone generator, flow meters, and four reaction columns. A schematic illustration of the setup is provided in Figure 1. The reaction columns were fabricated from polyvinyl chloride (PVC), each measuring 80 cm in height and 4.4 cm in internal diameter. The bottom of the carbon column was sequentially filled with support layers of 6 mm and 4 mm diameter glass beads to prevent loss of granular activated carbon due to inflow. The height of the glass bead layer was 5 cm, and the height of the activated carbon bed was 35 cm. The ozone reaction column was filled with 30 cm of glass beads to reduce ozone bubble size and ensure uniform gas distribution. Ozone was generated by the ozone generator and introduced from the bottom of the reaction column via flow meter control. Raw water was injected into the reaction column using a peristaltic pump, with an upflow mode of operation. Based on the flow rate at the flow meter outlet, the processes were divided into two processes: the traditional ozone-activated carbon process (O3-C process) and the integrated ozone-activated carbon process (O3/C process). The O3-C process simulated the existing ozone-activated carbon process in water plants, consisting of an ozone reaction column and an activated carbon reaction column. The O3/C process is also an improved ozone-activated carbon process. O3/C-1 and O3/C-2 are both O3/C processes with identical parameters, used for parallel experiment error analysis.

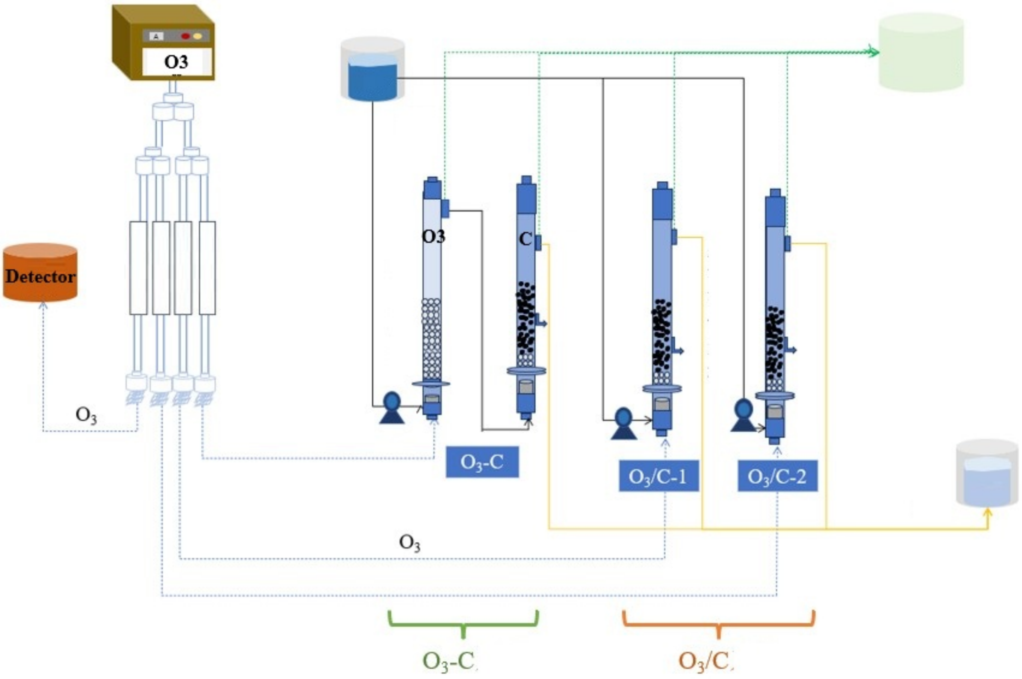

Figure 1 Schematic diagram of ozone activated carbon experimental device

Fresh activated carbon of equal mass was placed in both the O3-C and O3/C processes. The O3-C process consisted of an ozone reaction column and an activated carbon column. Ozone and raw water entered from the bottom of the ozone reaction column. After ozone oxidation in the ozone reaction column, the water exited from the top outlet and entered from the bottom of the activated carbon column. After treatment by activated carbon adsorption in the activated carbon column, the water was discharged from the top outlet of the activated carbon column. The O3/C process combined activated carbon and ozone in the same unit. Raw water and ozone entered through different inlets at the bottom of the ozone-activated carbon column. The raw water underwent simultaneous ozone oxidation and activated carbon adsorption inside the reaction column before exiting from the top outlet.

2.3 Ammonia Nitrogen Concentration Detection Method

Ammonia nitrogen was determined using a UV-Vis spectrophotometer. Exactly 0.03819 g NH_4Cl was transferred into a 1 L flask and brought to volume, yielding a 10 mg N L^{-1} reference. Aliquots of 0, 0.5, 1, 2, 4, 6, 8 and 10 mL were pipetted into 50 mL tubes and made up to the line to build the calibration set. These aliquots deliver 0–100 µg of NH_3-N. After adding 1 mL tartrate and 1 mL Nessler's solution, each tube is mixed and left for 10 min to develop color. Using ultrapure water as a blank control, use the spectral scanning mode of the UV spectrophotometer to scan in the wavelength range of 220~660 nm. Spectral scanning identified the absorption peak for NH_3-N at 420 nm. Measure the diluted ammonia nitrogen solutions at different gradient concentrations, and plot a standard curve using their absorbance.

2.4 Characterization Methods

(1) Specific Surface Area and Pore Size Distribution Analysis

The specific surface area and pore size distribution analyzer (BET model, SSA-4000, manufactured by Beijing Biaode Electronic Technology Co., Ltd.) was used to analyze the N_2 adsorption-desorption isotherm, specific surface area, pore volume, and pore size distribution of the activated carbon. Initially, the activated carbon sample underwent vacuum desorption for 2 hours to eliminate surface impurities. Subsequently, the specific surface area and related parameters of the activated carbon were determined by measuring the amount of N_2 adsorption and desorption at 77 K.

(2) Surface Functional Group Analysis

The surface functional groups of activated carbon at different adsorption stages were characterized using a Fourier transform infrared spectrometer (FT-IR, model FT-IR-6000, Tianjin Gangdong Technology Co., Ltd.). Alterations in surface groups were examined to investigate the reactions occurring during the adsorption process of the activated carbon. The activated carbon and potassium bromide were dried at 110°C for 2 hours, then ground and uniformly mixed at a mass ratio of potassium bromide to activated carbon of 500:1, followed by pellet formation under pressure. Accumulate 32 scans with a resolution of 4 cm^{-1} and a wavelength range of 4000~400 cm^{-1}.

(3) Surface Morphology Analysis

Scanning electron microscopy (SEM, Zeiss Sigma300) was used to scan fresh activated carbon and activated carbon at different adsorption times. First, the activated carbon was sputter-coated with gold using an ion sputter coater to improve the conductivity of the sample, with a processing time of 5 minutes. The SEM was then operated at 10 kV; images captured at escalating magnifications were used to track alterations in carbon topography, providing a visual proxy for pore evolution and sorption capacity.

3 Results and Discussion

3.1 Ammonia Nitrogen Removal Effec

As shown in Figure 2a and 2b, the ammonia nitrogen removal rates of the O3/C and O3-C processes during the initial and middle stages of operation fluctuated in the range of 3%~35%, with the maximum removal rate reaching 46%. The average ammonia nitrogen removal rates of the O3/C and O3-C processes were 16.36% and 15.5%, respectively. However, when the raw water ammonia nitrogen concentration was increased subsequently, the ammonia nitrogen removal effects of the O3/C and O3-C processes decreased. The removal rate of the O_3/C process varied between -3% and 17%, while that of the O_3-C process exhibited a broader fluctuation range from -13% to 29%, displaying no clear trend and even indicating that the ammonia nitrogen concentration in the ozone-treated effluent sometimes exceeded that of the influent. The low ammonia nitrogen removal efficiency of the O3/C and O3-C processes is mainly attributed to two aspects: ① The raw water concentration was low, and during the initial stage of experimental setup operation, the biofilm on the activated carbon surface had not yet formed. Ammonia nitrogen removal mainly relied on adsorption by the pores on the activated carbon surface, so the removal effects of the O3/C and O3-C processes on ammonia nitrogen were not manifested; ② The strong oxidizing property of ozone oxidizes other nitrogen-containing compounds in the water body into small molecule ammonia nitrogen, leading to situations where the ammonia nitrogen value in the main ozone effluent is higher than the influent ammonia nitrogen value during some periods, resulting in poor ammonia nitrogen removal effects by the O3/C and O3-C processes.

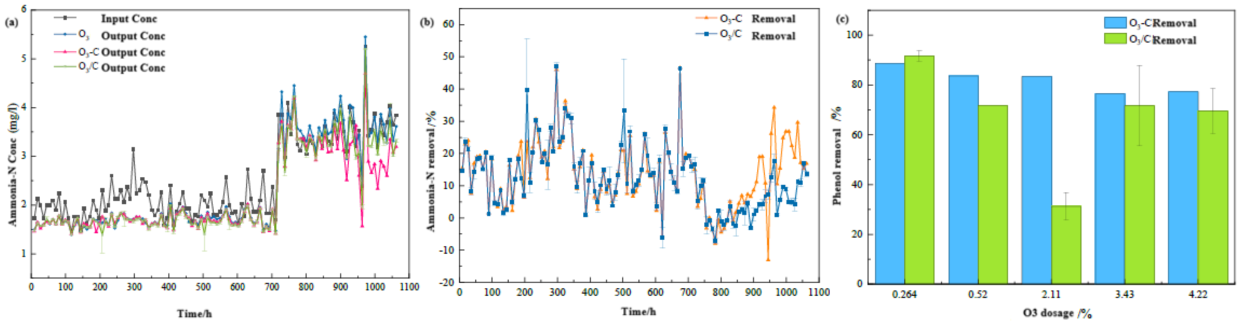

Figure 2 Effect of Two Processes on Removing Ammonia Nitrogen (a); Removal rate of ammonia nitrogen by two processes (b); Phenol removal rates of two processes under different ozone dosages (c)

Under the conditions of initial phenol mass concentration of 5-6 mg/L and pH 7, the effect of ozone dosage (O3 dosage rates of 0.264, 0.52, 2.11, 3.43, and 4.22 mg/min) on the degradation of phenol by ozone-activated carbon was investigated. The resulting phenol removal efficiencies are displayed in Figure 2c. As shown in the figure, the degradation performance of the O_3/C process for phenol initially decreased and then increased with rising ozone dosage, whereas the phenol degradation rate of the O_3-C process declined as the ozone dosage increased. The optimal ozone dosage for phenol removal by the O3/C and O3-C processes was 0.264 mg/min, with phenol removal rates of 92% and 89% for the O3/C and O3-C processes, respectively. The reason for the decrease in phenol degradation rate with increasing ozone dosage for both O3/C and O3-C processes is that the solubility of ozone is constant. Dosages higher than the optimal dose mean that the concentrations of hydroxyl radicals and ozone in the solution remain almost unchanged [14]. Therefore, the ozone dosage during experimental operation was set at 0.264 mg/min.

3.2 SEM Characterization of Surface Morphology

In the two combined processes, O3/C and O3-C, the combination methods of ozone and activated carbon are different. The integrated O3/C process brings ozone into direct contact with activated carbon, so ozone oxidation has a more direct impact on the activated carbon surface. Data show that this impact will change the pore structure, pore size, and surface elements of activated carbon to a certain extent. In the traditional O3-C process, ozone and activated carbon are separated into two independent units, so this contact impact is relatively small. This study used scanning electron microscopy to observe the surface structure of fresh activated carbon, activated carbon from the O3/C and O3-C reaction columns after 738 hours of operation, and activated carbon from the O3/C and O3-C reaction columns after 1737 hours of operation. The results are shown in Figure 3.

From Figure 3(a) and (b), it can be seen that the layered structure on the surface of fresh activated carbon is arranged neatly, the pores formed on different layers are clear and uniformly distributed in size, and there is no clogging by impurities in the pores, indicating that the fresh activated carbon has a huge specific surface area and good adsorption performance.

Panels c–d in Figure 3, recorded after 738 h of O_3/C operation, reveal a pore landscape that is virtually intact—channels even appear sharper. Continuous ozone scouring at the carbon interface apparently incinerates lodged organics on the fly, yielding in-situ surface renewal. This confirms the self-cleaning character of the O_3/C mode. In contrast, micrographs e–f of the sequential O_3–C train (738 h) display a starkly fouled façade—apertures are choked and the once-open porosity is no longer discernible versus virgin carbon. Between the various pore structures of the activated carbon, a large number of pollutant particles are adsorbed, and the surface properties have changed significantly. Figure 3(g) and (h) show the surface morphology of activated carbon in the O3/C process after 1737 hours of operation. It can be seen that the pore structure of the activated carbon is still as clear as initially, the surface is very clean, and the pores are distinct. Although some local breakage occurs on the activated carbon surface, reducing the smoothness, the overall structure of the activated carbon does not change much, and the overall morphology is not much different from fresh activated carbon.

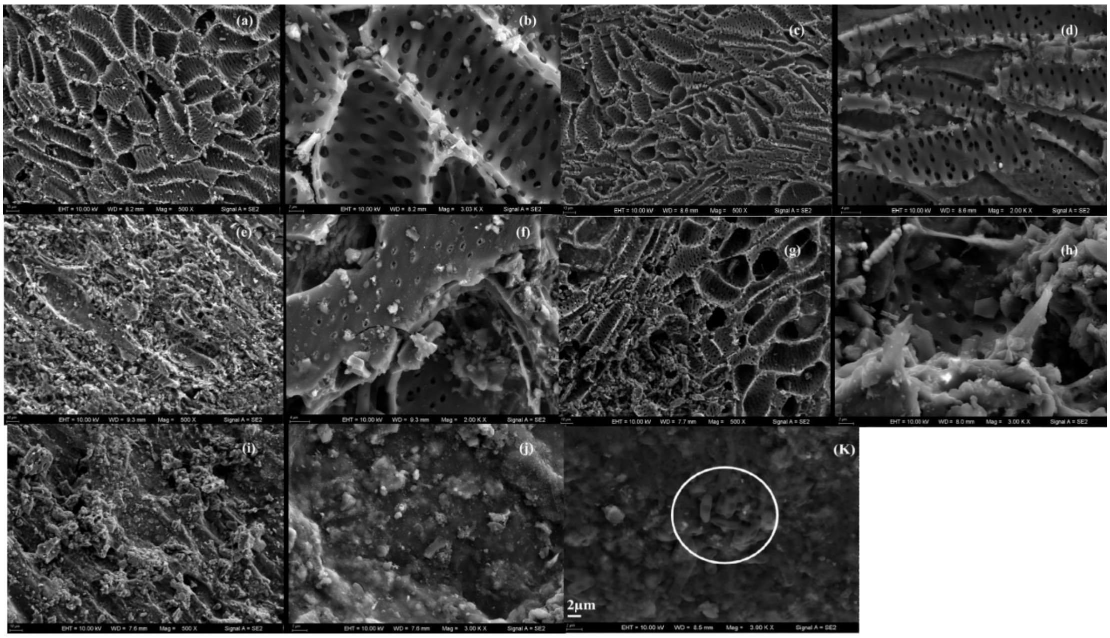

Figure 3 Scanning electron microscopy images of activated carbon surface under different operating times in O3/C and O3-C processes

In Figure 3(i) and (j), the surface of activated carbon in the O3-C process after 1737 hours of operation is almost completely covered by a dense, uniform layer of pollutants, making it impossible to distinguish the surface pore structure. This pollutant coverage layer appears to have a certain thickness and viscosity, so it may be composed of a mixture of biofilm and mud layer [15], containing organic matter, microbial degradation products, microorganisms, and other impurities. At this time, the activated carbon in the O3-C process has completely lost its adsorption performance. Instead, the biodegradation capacity of microorganisms covering the activated carbon surface may play a role. Figure 3(k) shows a further scan of the activated carbon surface in the O3-C process, revealing a large number of short rod-shaped bacteria on the surface of the O3-C process activated carbon. The ends of the bacterial cells are mostly blunt circles, with a size of about 1.3 μm. According to literature reports, Bacillus accounts for a high proportion in phenol-degrading bacterial genera. Therefore, during the removal of phenol as a micro-pollutant in this experiment, a large number of Bacillus may have grown on the activated carbon surface of the O3-C process. This also indicates that the traditional ozone-activated carbon process will inevitably transform into biological activated carbon, completely losing the adsorption function of activated carbon.

3.3 Changes in Surface Functional Groups of Activated Carbon

Figure 4 shows the Fourier transform infrared spectra of the surface functional groups of activated carbon from the O3/C and O3-C processes after 738 hours and 1493 hours of operation, obtained by infrared scanning. Compared with fresh activated carbon, changes in absorption peaks were observed at wavenumbers 1100, 1550, 1650, 2850, 3434, and 3800 cm^{-1}. The analysis is as follows:

(1) C≡C-H Stretching Vibration: Fresh carbon has multiple absorption peaks in the region of 3900~3600 cm^{-1}, caused by C≡C-H stretching vibration; the infrared spectra of activated carbon from the O3/C and O3-C processes after 738 h and 1493 h showed weakened absorption peaks in the region of 3900~3200 cm^{-1}, indicating a decrease in alkyne C≡C substances on the activated carbon surface during phenol removal. The absorption peaks

of O3-C process activated carbon after 1493 h were partially enhanced in the 3900~3200 cm^{-1} region but had not recovered to the level of fresh carbon.

(2) O-H Stretching Vibration Region: Absorption peaks in the range of 3600~3200 cm^{-1} indicate the presence of free hydroxyl groups, associated hydroxyl groups, or intermolecular hydrogen bonds, caused by O-H stretching vibration. Associated hydroxyl groups appear as strong, broad absorption bands between 3400~3200 cm^{-1}, while free hydroxyl groups typically show medium-intensity, sharp absorption peaks at 3650~3580 cm^{-1} [16]. As shown in the figure, the activated carbon from the O3/C and O3-C processes after 738 h and 1493 h has broad absorption peaks near 3434 cm^{-1}, indicating that the activated carbon surface may contain carboxyl or hydroxyl functional groups. The hydroxyl groups are mainly associated hydroxyls, with intermolecular hydrogen bonding playing an important role in the adsorption of aromatic compounds like phenol by activated carbon [17]. As the usage time of activated carbon increases, the absorption peaks weaken. The decrease in absorption peak intensity of O3-C process activated carbon is greater than that of O3/C process activated carbon, indicating that the intermolecular hydrogen bonding effect of O3/C process activated carbon on pollutants deactivated slowly.

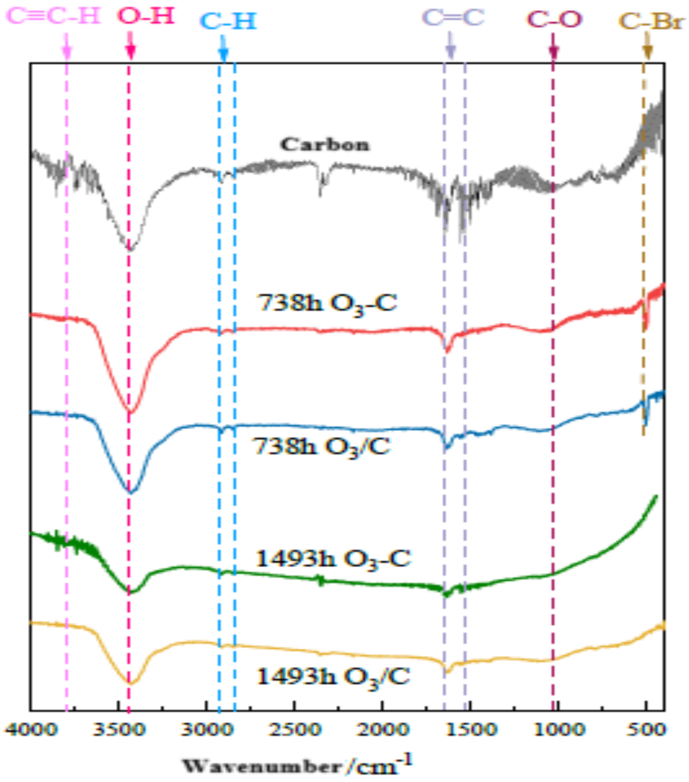

Figure 4 FT-IR spectra of activated carbon at different operating times

(3) C-H Stretching Vibration Region: Absorption peaks near 2920 cm^{-1}, close to 3000 cm^{-1}, are caused by saturated hydrocarbon C-H stretching vibration, indicating the presence of alkanes. The absorption peaks at 2920 cm^{-1} weakened for activated carbon from the O3/C and O3-C processes after 738 h and 1493 h.

(4) C=C Stretching Vibration: Fresh carbon, and activated carbon from the O3/C and O3-C processes after 738 h and 1493 h have absorption peaks near 1600 cm^{-1}. Taking 1600 cm^{-1} as the boundary, the absorption peaks to the left of 1600 cm^{-1} are caused by alkene C=C stretching vibration; to the right, there are absorption peaks, and there are multiple small absorption bands at 1600 cm^{-1}, 1558 cm^{-1}, 1500 cm^{-1}, and 1460 cm^{-1}, indicating the presence of aromatic hydrocarbons on the activated carbon. This is because the ring 内 C=C skeleton vibration of aromatic compounds causes aromatic ring skeleton vibration. Due to different substituents on the ring, the absorption peaks will vary. Furthermore, the spectrum of fresh activated carbon exhibits two absorption peaks near 1680 cm^{-1} and 1580 cm^{-1}, indicating that carbonyl groups on the carbon surface undergo conjugation with

aromatic rings. Carbonyl functional groups on activated carbon can attenuate the interaction between adsorbate and adsorbent [18]. The double peaks disappeared for O3-C process activated carbon after 738 h and 1493 h, indicating no conjugation reaction, which is more conducive to the adsorption function of activated carbon; the double peaks of O3/C gradually weakened, indicating a gradual reduction in conjugation reaction.

(5) C-O Stretching Vibration: Fresh carbon, activated carbon from the O3/C and O3-C processes after 738 h, and O3/C process activated carbon after 1493 h have absorption peaks in the region of 1300~1000 cm^{-1}, indicating the presence of alcohol or phenol functional groups. However, the absorption peaks in the 1300~1000 cm^{-1} region disappeared for O3-C process activated carbon after 1493 h, indicating changes in the types of surface functional groups of O3-C activated carbon.

(6) C-Br: The infrared spectra of activated carbon from the O3/C and O3-C processes after 738 h have absorption peaks near 500 cm^{-1}, indicating that the activated carbon adsorbed halogenated compounds.

From the above analysis, fresh carbon contains alkyne, intermolecular hydrogen bond, alkane, aromatic hydrocarbon, and alcohol or phenol functional groups. With prolonged operation, the intensity of the absorption peaks associated with the functional groups on the activated carbon gradually diminishes. The types and characteristics of the surface groups on activated carbon from the O_3/C and O_3-C processes did not exhibit significant changes. From the figure, after 1493 hours of operation, the absorption peaks in the C≡C-H stretching vibration region and the C=C stretching vibration region of O3/C process activated carbon recovered to some extent, indirectly indicating that the O3/C process has a regeneration effect on activated carbon.

3.4 Pore Volume

Figure 5 shows the changes in total pore volume and micropore volume of fresh activated carbon, activated carbon from the O3/C and O3-C processes after 738 hours of operation, and activated carbon from the O3/C and O3-C processes after 1737 hours of operation. It can be seen from the figure that compared with fresh activated carbon, the total pore volumes of activated carbon from the O3/C and O3-C processes after 738 hours of operation decreased by 57% and 52%, respectively, while the micropore volumes only decreased by 15% and 10%, respectively. However, after 1737 hours of operation, the total pore volumes of activated carbon from the O3/C and O3-C processes decreased by 73% and 85%, respectively, and the micropore volumes decreased by 19% and 77%, respectively.

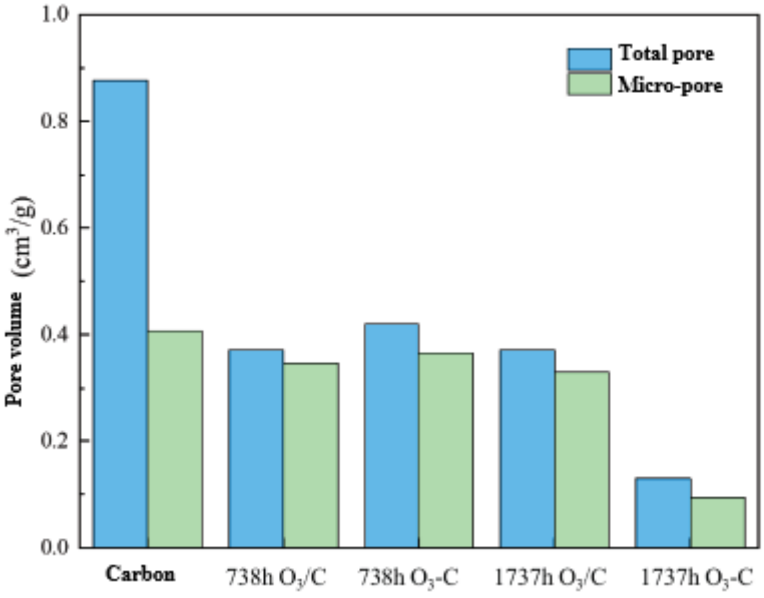

Figure 5 Comparison of pore volume of activated carbon with different operating times

With the operation time increases, the total pore volume of activated carbon decreases significantly, while the decrease in micropore volume is relatively small. Comparing the total pore volume and micropore volume of fresh activated carbon with that of activated carbon from the O_3/C and O_3-C processes after 738 hours of operation reveals that the reduction in total pore volume is primarily attributed to decreases in mesopore and macropore volumes, while the remaining pore structure is predominantly composed of micropores, with little change in micropore volume. Further comparison of the total pore volume and micropore volume of activated carbon from the O_3/C and O_3-C processes after 1737 hours of operation indicates that the total pore volume and micropore volume of activated carbon in the O_3/C process showed minimal change compared to those after 738 hours, with only a slight reduction in micropore volume. In contrast, the total pore volume and micropore volume of activated carbon in the O3-C process decreased drastically, almost losing the pore structure. This shows that in the traditional O3-C process, all pore structures of activated carbon are destroyed after long-term operation, leading to complete loss of adsorption capacity. Combined with the analysis of adsorption isotherms and specific surface area data, it can be concluded that as the operation time of activated carbon increases, the adsorption capacity, specific surface area, and pore volume of activated carbon in the O3/C process can remain relatively stable. Therefore, its adsorption capacity can remain stable for a long time, mainly due to the synchronous adsorption and regeneration effect of ozone on activated carbon under the combination of the O3/C process, extending the working cycle and service life of activated carbon and reducing process operating costs.

3.5 Catalytic Oxidation Mechanism

(1) Catalytic Reaction of Activated Carbon on Ozone

In the oxidation process of phenol by ozone, the indirect reaction rate between phenol ions and ozone molecules is 10^6 times faster than the direct reaction rate [19]. In the O3/C process, O3 can react with surface functional groups and inorganic substances of activated carbon [19], generating hydroxyl radicals (•OH), hydroperoxyl radicals (HO2•), and other oxygen-containing functional groups, as shown in Equations 1-2.

Additionally, dissolved ozone in water enters the pores on the activated carbon surface and, under the excitation of activated carbon, produces hydrogen peroxide (H2O2), as shown in Equation 3. The decomposition rate of this process is faster than the bulk decomposition rate of O3 in water catalyzed by OH-. Under acidic conditions, the activated carbon surface can stimulate ozone decomposition to produce •OH, while under neutral and alkaline conditions, H2O2 produced by O3 and activated carbon decomposes into •OH under the stimulation of alkaline groups on the activated carbon surface, as shown in Equation 4. Furthermore, the decomposition of H2O2 in water can produce additional HO2•. HO2• is a strong initiator of ozone decomposition, accelerating the decomposition of ozone in water, thereby improving the oxidation capacity of ozone.

O3+GAC→…→·OH （1）

O3+GAC→…→·O2H （2）

O3+GAC→…→H2O2 （3）

H2O2+GAC→…→·OH （4）

(2) Changes in Surface Properties and Pore Structure of Activated Carbon during Catalytic Reaction

From the above catalytic reaction equations of activated carbon, it is not difficult to see that during the catalytic reaction, activated carbon will have a certain loss, and ozone will also have a certain impact on the pore structure of activated carbon. To evaluate the destructive effect of ozone on activated carbon in the O3/C process, this study conducted a small-scale experiment to study the surface changes of activated carbon after long-term contact with ozone. Continuous direct oxidation of activated carbon by ozone leads to alterations in its pore structure. Compared to fresh activated carbon, after 144 hours of ozone contact, the specific surface area decreased by approximately 11.66%, the micropore specific surface area reduced by 20.00%, the mesopore specific surface area declined by 47.24%, the total pore volume diminished by 55.72%, and the micropore volume decreased by 14.84%. Consequently, ozone in the O_3/C process exerts a measurable impact on the properties of activated carbon, likely due to surface degradation caused by ozone oxidation. The structure of activated carbon after 144 hours of contact showed certain changes compared to fresh activated carbon. As the contact time between activated carbon and ozone increases, the micropore content ratio of activated carbon increases. This may be because ozone oxidation damages the macropore and mesopore structures on the activated carbon surface, gradually causing the loss of adsorption capacity of macropores and mesopores, or because ozone oxidation releases originally blocked or covered micropores inside and on the surface of activated carbon, leading to an increase in the proportion of active micropores.

The oxidation mechanism of phenol by •OH generated by ozone is: •OH attacks different positions of the benzene ring, producing intermediate products such as catechol and hydroquinone. •OH radicals further directly oxidize catechol and hydroquinone into small‑molecular acids such as formic acid, while para‑quinone undergoes hydroxylation followed by oxidation to form small‑molecular acids like oxalic acid. Finally, small molecular acids are oxidized to CO2 and H2O [20]. Synchronous regeneration of activated carbon by ozone, on the one hand, oxidizes pollutants adsorbed on the activated carbon surface through •OH and HO2• free radicals generated by O3 decomposition, generating intermediate products and ultimately producing CO2 and H2O; on the other hand, oxidizes microorganisms and biofilm on the activated carbon surface through O3, releasing the active sites on the activated carbon surface, effectively regenerating the activated carbon. The regeneration efficiency of activated carbon is influenced by ozone concentration. Higher ozone concentrations lead to a greater degree of oxidation on the activated carbon, resulting in an increased number of acidic functional groups (particularly carboxyl groups) on its surface [21]. Radical and other oxidizing species anchored on the carbon surface heighten its hydrophilicity and charge, accelerating the breakdown of sorbed organics [22] and thereby liberating vacant sites. At the same time, the generated oxygen-containing functional groups can also serve as active sites, promoting the decomposition of ozone stimulated by activated carbon, generating free radicals with strong oxidation capacity, as shown in Equation (5), forming a good cycle.

$$O3+HO2- +HO- \rightarrow \ldots \rightarrow \cdot OH \quad (5)$$

4 Conclusion

This paper analyzed the structure and pores of activated carbon from two processes after long-term operation through BET, SEM, EDS, and FT-IR, reviewed relevant literature on catalytic ozonation by ozone-activated carbon and the mechanism of synchronous adsorption regeneration by ozone-activated carbon, and then conducted a small-scale experiment on continuous contact between ozone and activated carbon to discuss the mechanism of synchronous adsorption regeneration by ultrasound-coupled ozone-activated carbon. The main conclusions are as follows:

(1) Through scanning electron microscopy (SEM) observation and analysis, the surface morphology and pore structure of activated carbon from the O_3/C process after 1737 hours of operation remained clear. The overall structure showed little change, and its general appearance was not significantly different from that of fresh activated carbon; the surface pore structure of activated carbon in the O3-C process is covered by a dense, uniform layer of pollutants, and a large number of short rod-shaped bacteria are present on the activated carbon surface, indicating that the traditional ozone-activated carbon process will inevitably transform into biological activated carbon, completely losing the adsorption function of activated carbon.

(2) Through FT-IR analysis, fresh carbon contains alkyne, intermolecular hydrogen bond, alkane, aromatic hydrocarbon, and alcohol or phenol functional groups. As the duration of use increases, the intensity of the absorption peaks associated with the functional groups on the activated carbon gradually diminishes. The various groups and properties of activated carbon from the O3/C and O3-C processes did not change significantly. After 1493 hours of operation, the absorption peaks in the C≡C-H stretching vibration region and the C=C stretching vibration region of O3/C process activated carbon recovered to some extent, indirectly indicating that the O3/C process has a regeneration effect on activated carbon.

(3) Based on BET analysis, after 1737 hours of operation, the decrease in micropore specific surface area of the

activated carbon in the O_3/C process was minor, while the relative reduction in mesopore specific surface area was more pronounced. Compared to the activated carbon after 738 hours of operation, the changes in total pore volume and micropore volume were not substantial, with only a slight decrease observed in micropores. In contrast, for the activated carbon in the O_3-C process, both the micropore and mesopore specific surface areas decreased significantly, and the total pore volume and micropore volume declined drastically, nearly resulting in the loss of the pore structure. The activated carbon in the O_3/C process was able to maintain adsorption capacity comparable to its initial state, whereas the adsorption capacity of the activated carbon in the O_3-C process decreased by nearly 75%, almost completely losing its adsorptive properties.

(4) In the O3/C process, O3 can react with surface functional groups and inorganic substances of activated carbon to generate •OH, HO2•, and other oxygen-containing functional groups. Dissolved ozone in water produces H2O2 under the excitation of activated carbon, and H2O2 produced by O3 and activated carbon decomposes into •OH under the stimulation of alkaline groups on the activated carbon surface. Aqueous H_2O_2 decomposes to HO_2•, a potent trigger that propels O_3 breakdown; this cascade amplifies the overall oxidative potential of the system.

(5) As the contact time between activated carbon and ozone increases, the micropore content ratio of activated carbon increases. Hence, the intimate presence of ozone in the O_3/C setup inevitably reshapes the carbon’s surface chemistry. Synchronous regeneration of activated carbon by ozone generates a large amount of •OH through O3, oxidizing pollutants adsorbed on the activated carbon surface, generating intermediate products, and ultimately producing CO2 and H2O; Meanwhile, ozone assaults the microbial lawn and biofilm cladding the carbon, stripping them away to reopen active patches and, in effect, self-regenerate the sorbent. The regeneration efficiency of activated carbon is influenced by ozone concentration. Higher ozone concentrations result in a greater degree of oxidation on the activated carbon surface. Furthermore, the oxygen-containing functional groups generated by the reaction of O_3 with the activated carbon can also act as active sites, promoting the decomposition of ozone catalyzed by the activated carbon. This process produces highly oxidative free radicals, establishing a beneficial cycle for regeneration.

References

[1] BRILLAS E, SIRéS I, OTURAN M A. Electro-Fenton process and related electrochemical technologies based on Fenton’s reaction chemistry [J]. Chemical reviews, 2009, 109(12): 6570-631.

[2] GIBBONS J, LAHA S. Water purification systems: a comparative analysis based on the occurrence of disinfection by-products [J]. Environmental Pollution, 1999, 106(3): 425- 428.

[3] QIANG Z, LING W, TIAN F. Kinetics and mechanism for omethoate degradation by catalytic ozonation with Fe (III)-loaded activated carbon in water [J]. Chemosphere, 2013, 90(6): 1966-1972.

[4] CHU W, MA C W. Quantitative prediction of direct and indirect dye ozonation kinetics [J]. Water research, 2000, 34(12): 3153-3160.

[5] SINGER P C. Control of disinfection by-products in drinking water [J]. Journal of environmental engineering, 1994, 120(4): 727-744.

[6] SONG S, LIU Z, HE Z, et al. Degradation of the biocide 4-chloro-3, 5-dimethylphenol in aqueous medium with ozone in combination with ultraviolet irradiation: operating conditions influence and mechanism [J]. Chemosphere, 2009, 77(8): 1043-1051.

[7] ANDREADAKIS A D, MAMAIS D, GAVALAKIS E A, et al. Removal of taste and odour from potable water by ozone and powdered activated carbon (PAC) [J]. International Journal of Environment and Waste Management, 2010, 5(3-4): 392-409.

[8] ALATON I A, BALCIOGLU I A, BAHNEMANN D W. Advanced oxidation of a reactive dyebath effluent: comparison of O3, H2O2/UV-C and TiO2/UV-A processes [J]. Water research, 2002, 36(5): 1143-1154.

[9] ZHENG J, LIN T, CHEN W, et al. Removal of precursors of typical nitrogenous disinfection byproducts in ozonation integrated with biological activated carbon (O3/BAC) [J]. Chemosphere, 2018, 209: 68-77.

[10] HE Z W, WANG F, ZOU Z S, et al. Recent advances and perspectives in roles of humic acid in anaerobic digestion of waste activated sludge [J]. Chemical Engineering Journal, 2023, 466: 143081.

[11] FENG J, ZHANG X, FU J, et al. Catalytic ozonation of oxalic acid over rod-like ceria coated on activated carbon [J]. Catalysis Communications, 2018, 110: 28-32.

[12] ZHAO Y, LIN S, CHOI J W, et al. Prediction of adsorption properties for ionic and neutral pharmaceuticals and pharmaceutical intermediates on activated charcoal from aqueous solution via LFER model [J]. Chemical Engineering Journal, 2019, 362: 199-206.

[13] ZHAO X, ZENG X, QIN Y, et al. An experimental and theoretical study of the adsorption removal of toluene and chlorobenzene on coconut shell derived carbon [J]. Chemosphere, 2018, 206: 285-292.

[14] ALVAREZ P M, GARCIA-ARAYA J F, BELTRáN F J, et al. The influence of various factors on aqueous ozone decomposition by granular activated carbons and the development of a mechanistic approach [J]. Carbon, 2006, 44(14): 3102-3112.

[15] VALDéS H, SáNCHEZ-POLO M, RIVERA UTRILLA J, et al. Effect of ozone treatment on surface properties of activated carbon [J]. Langmuir, 2002, 18(6): 2111-2116.

[16] DE OLIVEIRA T F, CHEDEVILLE O, FAUDUET H, et al. Use of ozone/activated carbon coupling to remove diethyl phthalate from water: Influence of activated carbon textural and chemical properties [J]. Desalination, 2011, 276(1-3): 359-365.

[17] Ke X, Liu C, Tang S Q, et al. Characterization of Acinetobacter indicus ZJB20129 for heterotrophic nitrification and aerobic denitrification isolated from an urban sewage treatment plant [J]. Bioresource Technology, 2021, 347: 126423.

[18] WANG Y, LI L, DONG H, et al. Removal of carbonaceous and nitrogenous disinfection by-product precursors in biological activated carbon process of drinking water: Is service life a pivotal factor [J]. Chemical Engineering Journal, 2023, 465: 142875.

[19] LIU Y, HAN Y, ZHANG J, et al. Deciphering effects of humic acid in landfill leachate on the simultaneous nitrification, anammox and denitrification (SNAD) system from performance, electron transfer and microbial community [J]. Science of the Total Environment, 2022, 809: 151178.

[20] WANG C, GALLAGHER D L, DIETRICH A M, et al. Data analytics determines co-occurrence of odorants in raw water and evaluates drinking water treatment removal strategies [J]. Environmental Science & Technology, 2021, 55(24): 16770-16782.

[21] AKCAALAN R, DEVESA-GARRIGA R, DIETRICH A, et al. Water taste and odor (T&O): Challenges, gaps and solutions from a perspective of the WaterTOP network [J]. Chemical Engineering Journal Advances, 2022, 12: 100409.

[22] REN X, WU Q, SHU J, et al. Efficient removal of organic matters and typical odor substances in rural drinking water using Ozone-BAC-UF combined system to meet new water quality standards in China [J]. Separation and Purification Technology, 2023, 327: 124899.